JOURNAL OF MATERIALS SCIENCE 20 (1985) 3375 – 3384

Scanning electron microscopy studies on failure of filled polychloroprene

D. K. SETUA, S. K. DE
Rubber Technology Centre, Indian Institute of Technology, Kharagpur 721302, India

Scanning electron microscopy (SEM) studies of the effect of particulate fillers (silica and carbon black) and short fibres (silk) on the fracture surface morphology of polychloroprene vulcanizates failed under tension, tear, abrasion and flexing have been made. It has been observed that the type of failure testing and the nature of the filler cause drastic changes in the fractographs. An attempt has been made to correlate these changes with the strength of polychloroprene vulcanizates.

1. Introduction

Some important factors contributing towards failure of rubber products are tensile and tear fracture, wear, hysteresis and mechanical fatigue. Significant improvement in the strength of rubbers can be obtained by incorporating appropriate fillers. It would be interesting, therefore, to study how the fracture surfaces depend on the failure mode and nature of fillers. De and co-workers [1–6] have utilized SEM as a tool in such studies.

Polychloroprene, because of its high chemical and weather resistance, heat resistance and acceptable range of physical properties, finds a wide range of applications. However, little is known about its failure behaviour. In this paper we report results of our SEM studies on fracture surfaces failed under tension, tear, abrasion and flexing. Secondly, we have also studied the effect of reinforcing particulate fillers and short fibres on the failure behaviour. Short fibres, in contrast to particulate fillers, are known to produce mechanical anisotropy in rubber vulcanizates [7–9]. In this paper, we have studied composites in which the short fibres are aligned in the longitudinal direction. Semi-reinforcing carbon black (FEF-N 550) and Vulcasil-S were chosen as particulate fillers and silk fibres as the short fibres.

2. Experimental procedure

Formulations of the mixes, their processing characteristics, and the physical properties of the corresponding vulcanizates are given in Table I, II and III respectively. Mixing was done on a conventional laboratory open mill (150 × 330 mm) at 30 to 40° C according to ASTM designation D 15-70. Nip gap, mill roll speed ratio and the time of mixing were kept the same for all the mixes. The compounds were vulcanized to their respective optimum cure times, determined by Monsanto rheometer (R-100) at 150° C. The details of preparation of the vulcanizates are described in our previous publications [4, 7, 8]. In the case of short silk fibre-filled compounds, the fibres were first separated from undesirable foreign matter and chopped to 6 mm length. The different ingredients were added to the mixes according to the sequence given in Table I. The extent of fibre breakage due to mixing was determined by dissolving the compound in chloroform, followed by extraction of the fibres and examination of fibre length distribution by an optical polarizing microscope (Model, Leitz HM-Pol) under reflected light. A fall in the mean aspect ratio from its original value of 500 to 85 after mixing was observed.

The stress–strain properties, tensile strength, elongation at break, modulus and tear strength of the vulcanizates were measured on a "Zwick" tensile testing machine at room temperature (30° C). The rate of separation of the grips for

0022–2461/85 $03.00 + .12

TABLE I Formulations of the mixes

Ingredient	Content of the mix (parts by wt)			
	A	B	C	D
Polychloroprene[a]	100	100	100	100
MgO[b]	4	4	4	4
PBNA[c]	2	2	2	2
Silica[d]	–	40	–	–
Carbon black[e]	–	–	40	10
Processing oil	–	–	4	1
Silk fibre[f]	–	–	–	20
Cohedur RK[g]	–	–	–	10
Stearic acid	0.5	0.5	0.5	0.5
ZnO	5	5	5	5
Cohedur A[h]	–	–	–	3.2
TMTM[i]	1	1	1	1
DOTG[j]	0.5	0.5	0.5	0.5
Sulphur	0.5	0.5	0.5	0.5

[a] Neoprene rubber, WM-1 grade supplied by Bengal Waterproof Ltd, Panihati, Calcutta.
[b] Magnesia, neoprene grade, supplied by Bengal Waterproof Ltd, Panihati, Calcutta.
[c] Phenyl β-naphthylamine (Accinox DN), supplied by Alkali and Chemical Corporation of India Ltd, Rishra.
[d] Vulcasil-S, supplied by Bata India Ltd, Calcutta.
[e] Semi-reinforcing carbon black (FEF-N 550), supplied by Phillips Carbon Black Ltd, Durgapur.
[f] Silk fibre (Mulberry type), obtained as waste in filatures of Silk Khadi Mondol, Bishnupur, West Bengal.
[g] A condensation product of resorcinol and formaldehyde, obtained from Bayer India Ltd, Bombay.
[h] Methoxy methyl melamine, obtained from Bayer India Ltd, Bombay.
[i] Tetramethyl thiuram monosulphide, supplied by Alkali and Chemical Corporation of India, Ltd, Rishra.
[j] Di-*ortho*-tolyl guanidine, supplied by Bengal Waterproof Ltd, Panihati, Calcutta.

the above tests was adjusted to 500 mm min^{-1}. ASTM procedures were adopted in the determination of physical properties. The procedures for determining processing characteristics like mill shrinkage, Mooney viscosity and Mooney scorch time (at 120° C) and the green strength of the compounds by the method suggested by Foldi have been described earlier [7, 8].

The shapes of the tensile and tear test specimens along with the direction of application of force, fracture surfaces obtained after failure and the scan areas used for SEM observations are depicted in Fig. 1. Fig. 2 shows the shapes of test specimens used in Du Pont abrasion and De Mattia flexing tests. The mode of testing and the portion of the failed specimen used for SEM studies have also been shown in this figure. The fracture surfaces were sputter-coated with gold within 24 h of testing. SEM studies were carried out using a Philips (Model, 500) scanning electron microscope. The orientation of the photographs was kept constant for a particular mode of testing and the tilt was adjusted to 0° in all cases.

TABLE II Processing characteristics

Property	Mix			
	A	B	C	D
Mooney scorch time at 120° C, T_5 (min)	28.0	26.0	22.0	10.5
Mooney viscosity ML (1 + 4) at 120° C	27	118	60	37
Mill shrinkage (%)	56.0	38.0	22.0	1.5
Green strength (MPa)	–	3.03	0.84	3.25
Optimum cure time at 150° C (min)	34.0	33.5	31.0	30.0

3. Results and discussion

3.1. Processing characteristics

Although optimum cure times do not show significant changes on addition of different fillers, Mooney scorch time, Mooney viscosity, mill shrinkage and green strength were found to depend on the filler. Short fibre-filled polychloroprene showed maximum scorchiness and lowest mill shrinkage, while silica-filled compound showed highest Mooney viscosity. Both fibre and silica-filled compounds showed high green strength. The low mill shrinkage and high green strength of fibre-filled compound have been reported earlier [7–9].

3.2. Physical properties

Hardness and heat built-up of the vulcanizates increase on addition of fillers. Fibre-filled composite shows maximum hardness while the silica-filled vulcanizate shows maximum heat build-up. Addition of reinforcing fillers increases tear resistance and the highest increase is noted in the case of silica-filled vulcanizate. As expected, resilience decreases on addition of fillers and the decrease is maximum in the case of silica. But the increase in tensile strength is maximum in the case of silica while addition of fibre up to 20 phr (parts per hundred of rubber) lowers the tensile strength.

Elongation at break decreases on addition of fillers, namely carbon black and short fibres and the decrease is remarkable in the case of fibre-filled composite (unfilled 910%, fibre 30%).

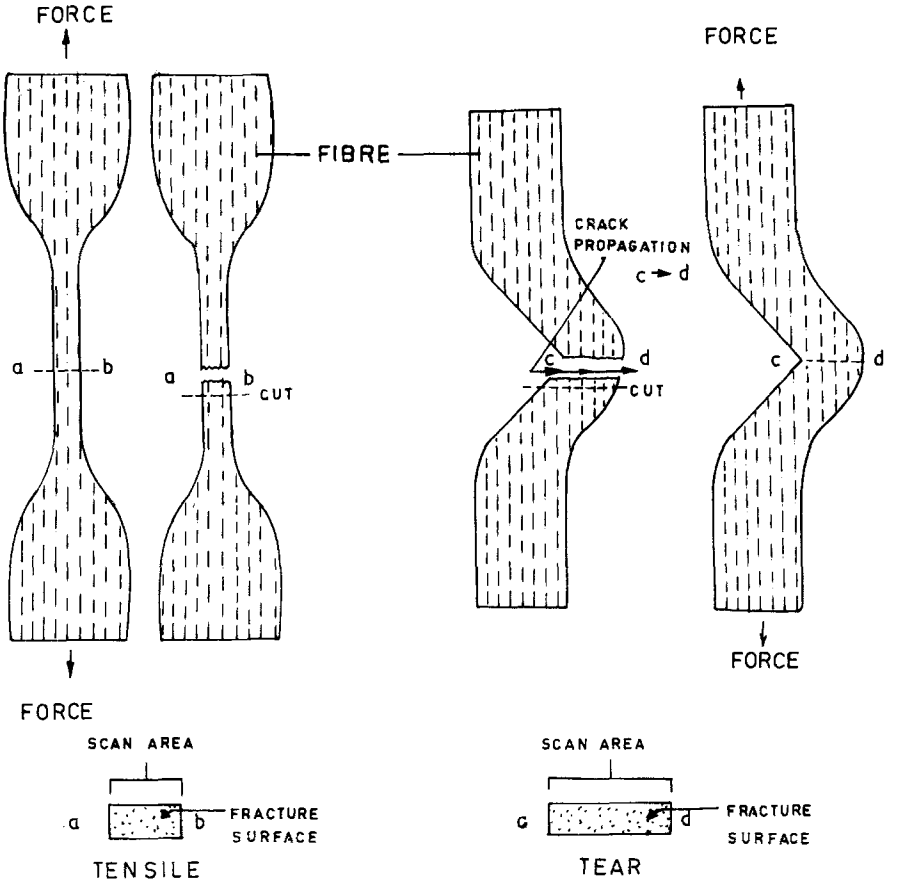

Figure 1 Shapes of the tensile and tear test specimens with longitudinal fibre orientation, mode of testing, corresponding fracture surfaces and scan areas.

TABLE III Physical properties of the vulcanizates

Property	Vulcanizate			
	A	B	C	D
Hardness, Shore A	50	82	74	90
Resilience (%)	69	47	57	53
Heat build-up (ΔT) for 20 min at 50° C (° C)	21	56	32	39*
Tear strength ($kN\,m^{-1}$)	21.5	77.7	40.8	43.0
Tensile strength (MPa)	14.85	22.42	19.76	9.61
Elongation at break (%)	910	940	450	30
Modulus at 100% elongation (MPa)	0.11	1.13	2.03	–
Modulus at 300% elongation (MPa)	0.48	3.34	13.25	–
Compression set at constant stress (400 lb) (%)	15	18	7	9
Compression set at constant strain (25%) (%)	35	57	23	46
Permanent set (%)	3	22	2	–
Flex cracking resistance (k cycles)	8.5	42	> 200	2.2
Abrasion loss ($ml\,h^{-1}$)	4.19	1.65	1.23	1.98

*Result at 15 min beyond which sample was blown out.

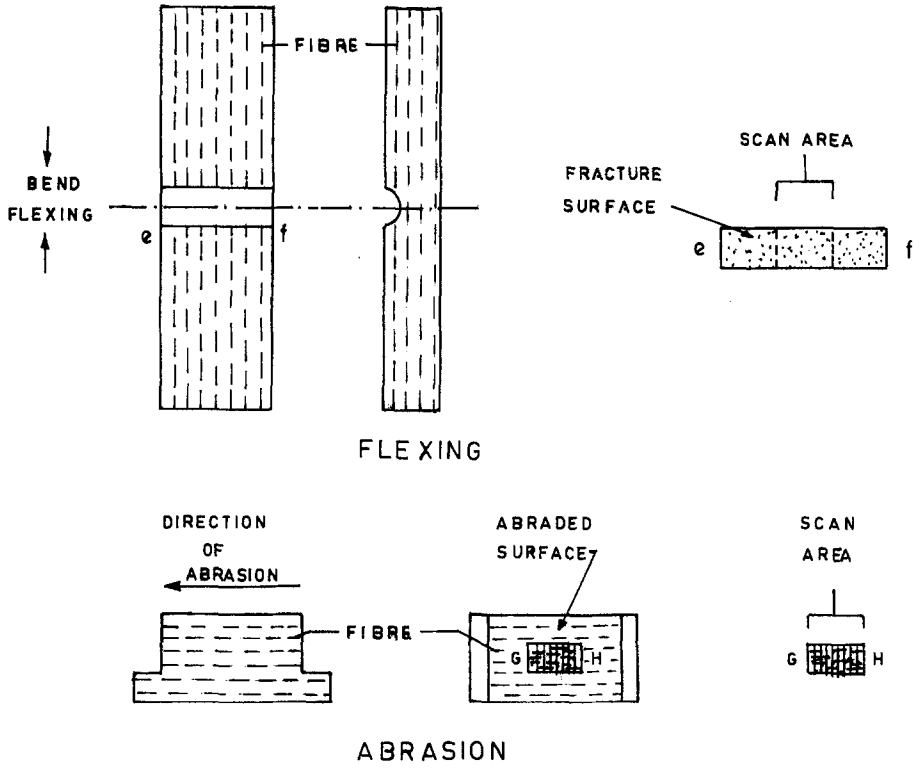

Figure 2 Shapes of the Du Pont abrasion and De Mattia flexing test specimens with longitudinal fibre orientation, mode of testing, corresponding fracture surfaces and scan areas.

However, the silica-filled vulcanizate shows high elongation at break due to the mobility of polymer chains on the filler surface [10–13]. For similar reasons the set properties are poor in silica-filled vulcanizate. Stress–strain curves for different vulcanizates are shown in Fig. 3. Modulus values are maximum in the case of carbon black-filled vulcanizate presumably due to high polymer–filler interaction. Flex cracking resistance decreases on addition of short fibres, but increases on addition of particulate fillers and the increase is maximum in the case of carbon black-filled vulcanizate. Abrasion resistance increases on the addition of fillers and the increase is maximum in the case of carbon black. While changes in physical properties on addition of carbon black and silica are expected [14–20], the changes in physical properties for silk fibre-filled composite are similar to that in other short fibre–rubber systems [7–9, 21–23].

3.3. Scanning electron microscopy studies

3.3.1. Tensile fracture surface

Fig. 4 is the scanning electron micrograph of the tensile fracture surface of unfilled vulcanizate of Mix A. It shows the presence of a rough zone at one end of the fracture surface preceded by a comparatively smooth region. It appears that this feature is characteristic of unfilled vulcanizates of strain crystallizing elastomers, since similar observations have been made earlier in the case of sulphur cured unfilled natural rubber vulcanizates [2]. However, the presence of cracks across the entire surface in the smooth region, as shown in Fig. 5, accounts for the lower tensile strength of unfilled polychloroprene vulcanizate of Mix A as compared to that of unfilled natural rubber vulcanizates.

The improvement in tensile strength on the addition of carbon black (Mix C) is also reflected in the nature of the surface morphology as shown in Fig. 6, which is the scanning electron micrograph of tensile fracture surface of Mix C. The high level of polymer–filler interaction in this case causes the formation of regions of high strength in the vulcanizate and hence smooth propagation of fracture is hindered. This results in the occurrence of a rough fracture surface and short tear lines.

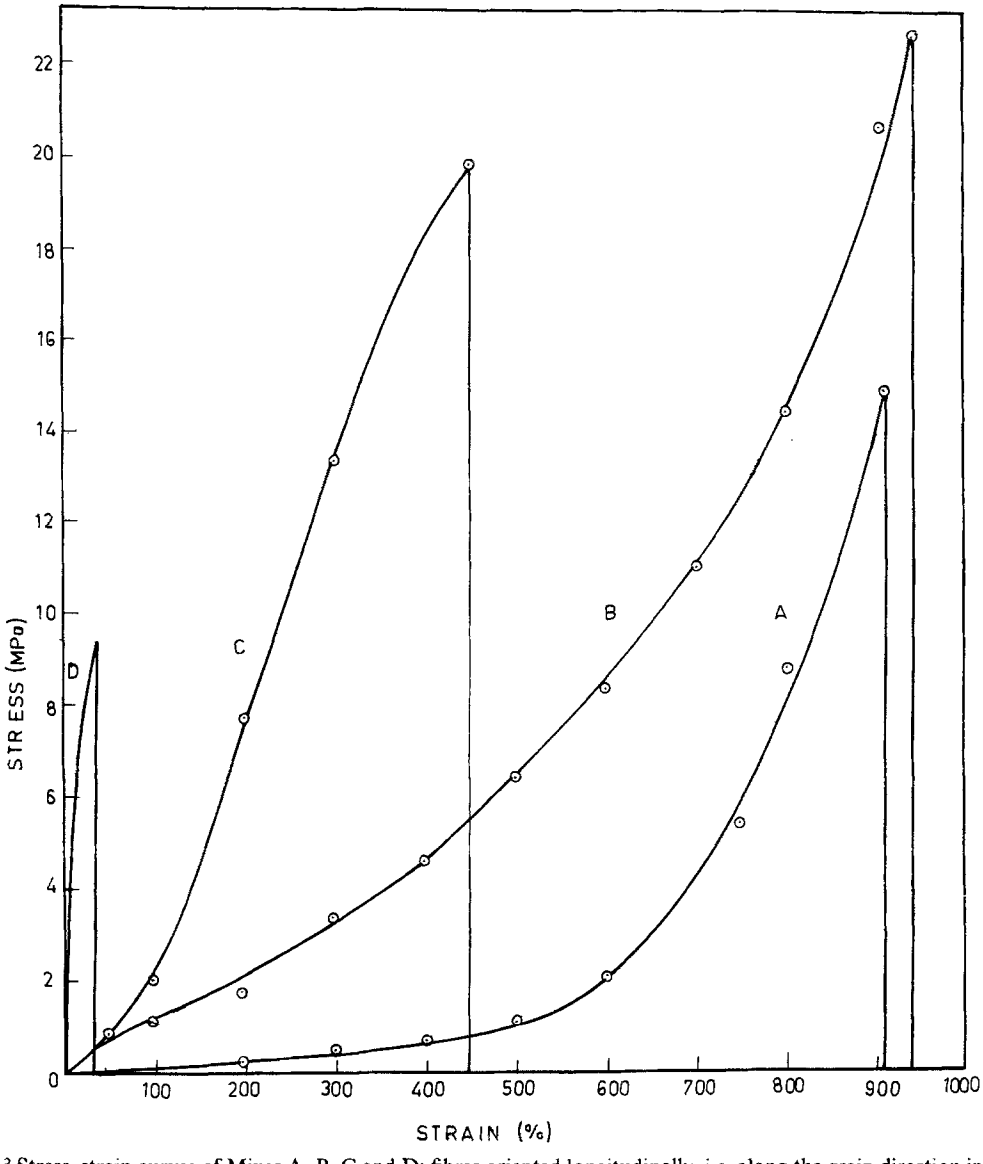

Figure 3 Stress–strain curves of Mixes A, B, C and D; fibres oriented longitudinally, i.e. along the grain direction in Mix D.

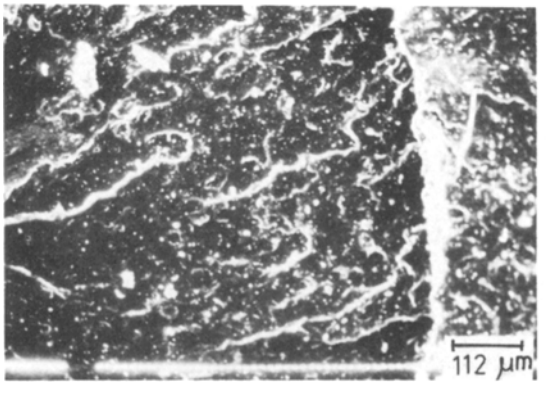

Figure 4 Scanning electron micrograph of the tensile fracture surface of Mix A.

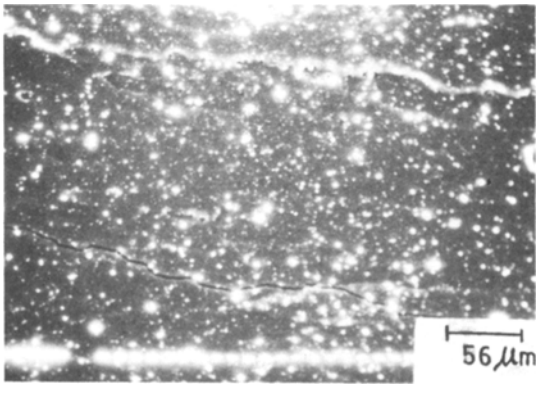

Figure 5 Scanning electron micrograph of the tensile fracture surface of Mix A.

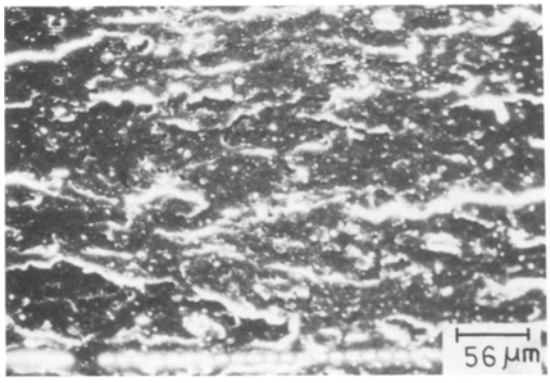

Figure 6 Scanning electron micrograph of the tensile fracture surface of Mix C.

Figure 8 Scanning electron micrograph of the tensile fracture surface of Mix D.

The fracture surface topography of silica-filled vucanizate (Mix B) is similar to that of carbon black-filled vulcanizate (Mix C). However, the short tear lines in Mix B (Fig. 7) are curved and the fracture surface shows the presence of some silica aggregates.

Fibre-filled composite (Mix D), on the other hand, exhibits very different characteristics in the fractograph. Owing to increased hardness, the composite becomes brittle and deep cracks develop (Fig. 8). When the fibres are properly bonded to the rubber matrix, application of tensile stress results in the breakage of fibres. On the other hand, pulling out of the fibres occurs when the fibres are not sufficiently bonded to the rubber matrix. The large number of loose fibres and holes on the fracture surface (Fig. 8) imply extensive debonding and pulling out of the fibres from the rubber matrix. Thus, as a result of poor fibre–rubber adhesion, pulling out of the fibres predominates over fibre breakage. The development of deep cracks in addition to extensive fibre–rubber debonding leads to poor tensile strength in Mix D.

3.3.2. Tear fracture surface

A scanning electron micrograph of the tear fracture surface of the vulcanizate of Mix A is shown in Fig. 9. Smooth propagation of the fracture front due to lower hindrance offered by the unfilled vulcanizate to the advancing tear leads to the generation of many steady tear lines and a broad steady tear path. Similar features on the tear fracture surface of unfilled vulcanizates have also been found in the case of sulphur-cured natural rubber vulcanizates [1, 24]. These features are indicative of poor tear strength. This is in keeping with the experimental observation of a low tear strength of this vulcanizate (Mix A).

Fig. 10 shows a scanning electron micrograph of the tear fracture surface of carbon black-filled

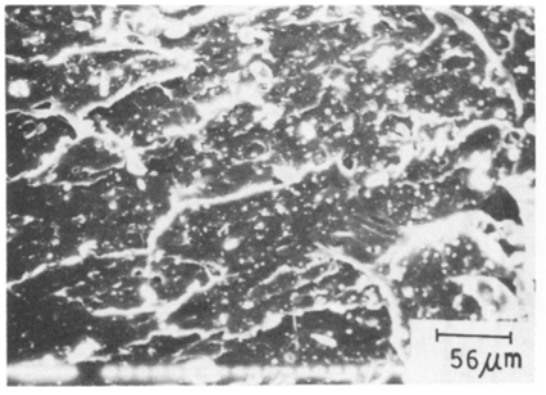

Figure 7 Scanning electron micrograph of the tensile fracture surface of Mix B.

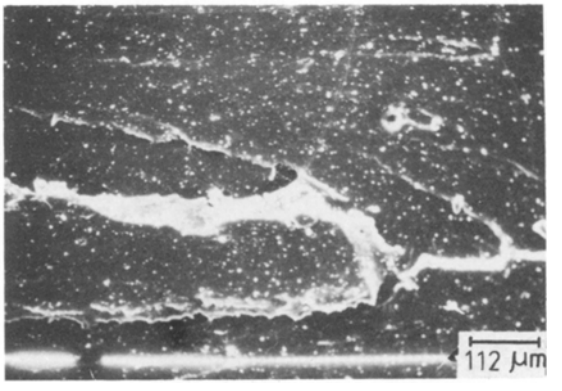

Figure 9 Scanning electron micrograph of the tear fracture surface of Mix A.

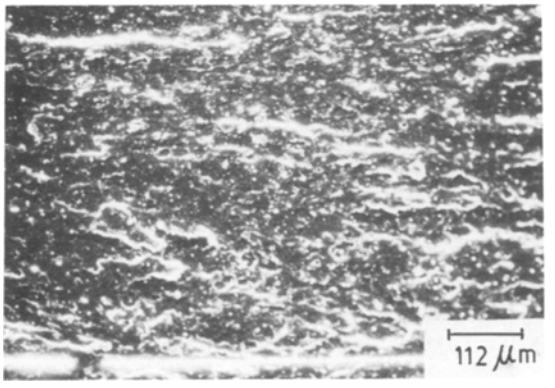

Figure 10 Scanning electron micrograph of the tear fracture surface of Mix C.

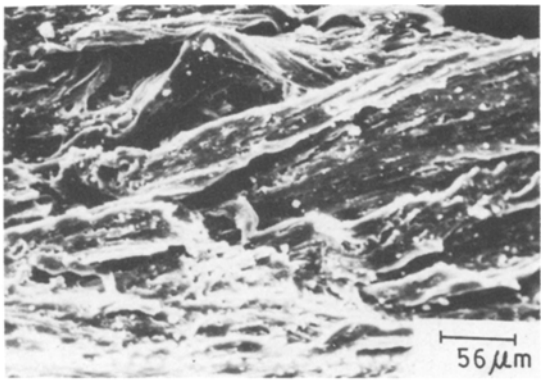

Figure 12 Scanning electron micrograph of the tear fracture surface of Mix B.

vulcanizate of Mix C. Carbon black provides improved wetting and adhesion properties and prevents the tear paths from proceeding straight. The micrograph shows a number of short tear lines randomly distributed over a relatively coarse surface as on the tensile fracture surface (Fig. 6).

The surface topography of the tear fracture surface of the silica-filled vulcanizate of Mix B (shown in Figs. 11 and 12) is very different from those of vulcanizates of Mixes A and C. High elongation and high set of the matrix lead to fibril formation (Fig. 11). Extensive deformation as well as folding of the surface are observed at higher magnification (Fig. 12). All these features are in conformity with our experimental observation of high tear strength of this vulcanizate.

As shown in Fig. 13, fibre-filled composite (Mix D) shows no tear line on the fracture surface. Fibres physically obstruct the propagating tear path by deviating the fracture front imparting thereby a higher resistance to the propagating tear. This increases the tear strength to the same level as in carbon black-filled vulcanizate. Absence of tear lines on the fracture surface are characteristic features of this fractograph. Similar observations have been made earlier [8, 21].

3.3.3. Abraded surface

Fig. 14 shows a scanning electron micrograph of the abraded surface of unfilled vulcanizate of Mix A. The figure shows extensive material displacement from left to right which is also the direction of application of frictional force experienced by the specimen surface when sliding against the abrasive wheel. Low tear strength and consequent ease of crack growth in the abrasion test specimens results in high abrasion

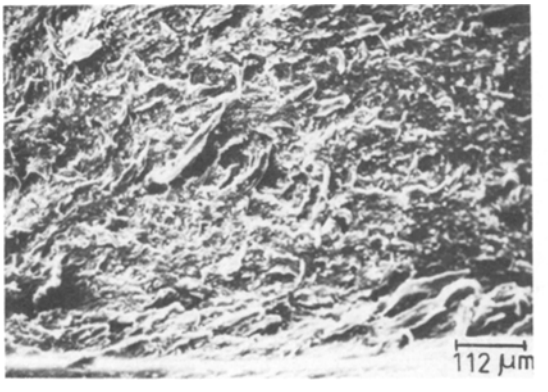

Figure 11 Scanning electron micrograph of the tear fracture surface of Mix B.

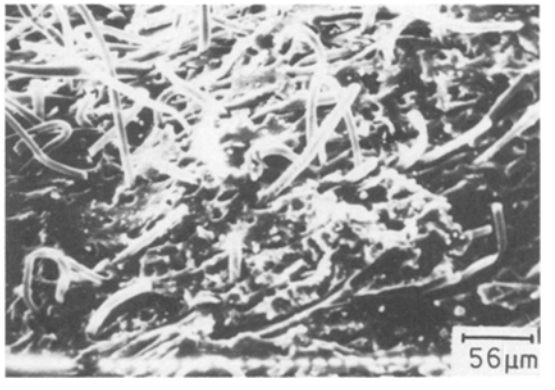

Figure 13 Scanning electron micrograph of the tear fracture surface of Mix D.

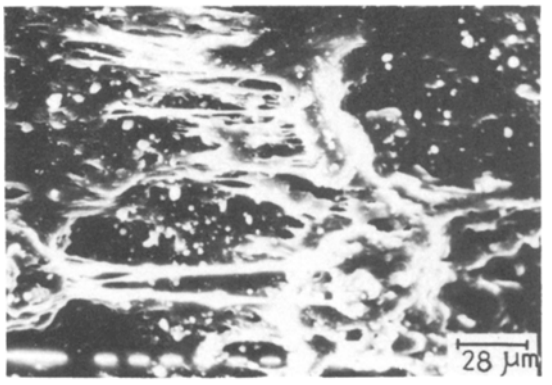

Figure 14 Scanning electron micrograph of the abraded surface of Mix A.

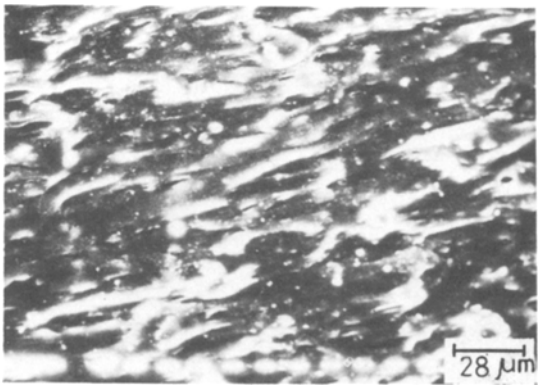

Figure 16 Scanning electron micrograph of the abraded surface of Mix C.

loss for this vulcanizate. Studies on the application of fracture mechanics to explain abrasion of rubber vulcanizates by Southern and Thomas [25] also support this observation.

Abrasion resistance is improved remarkably on the addition of reinforcing fillers such as carbon black or silica in the mixes. The scanning electron micrographs of the abraded surfaces in these cases are also different from that obtained in the case of unfilled vulcanizate. The scanning electron fractograph of the silica-filled vulcanizate of Mix B (Fig. 15), as expected, shows a lesser extent of material displacement and longer fibrils. The abraded surface of carbon black-filled vulcanizate of Mix C shows least material removal and negligible fibril formation (Fig. 16).

Short fibre–polychloroprene composite (Mix D) shows quite different characteristics. Broken fibres and agglomerated mass along with grooves are observable on the surface (Fig. 17), but no fibril formation takes place and regular channels exist. Higher abrasion loss of Mix D compared to Mixes B and C is, therefore, expected.

3.3.4. Flex failed surface.

Fig. 18 is the scanning electron micrograph of flex failed surface of unfilled vulcanizate of Mix A. Brittle failure with extensive cracking over the surface in this case supports the very low flex cracking resistance of this vulcanizate.

In contrast to natural rubber vulcanizates [3], polychloroprene vulcanizates show increased flex cracking resistance on the addition of fillers to the mixes. Extensive matrix flow and absence of cracks, observed in Fig. 19, give rise to very high flex cracking resistance of the carbon black-filled vulcanizate of Mix C. Silica-filled vulcanizate (Mix B), on the other hand, undergoes

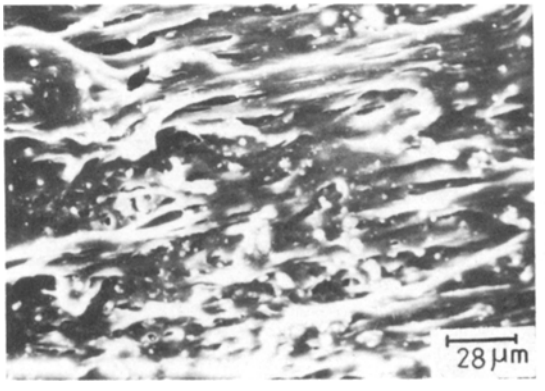

Figure 15 Scanning electron micrograph of the abraded surface of Mix B.

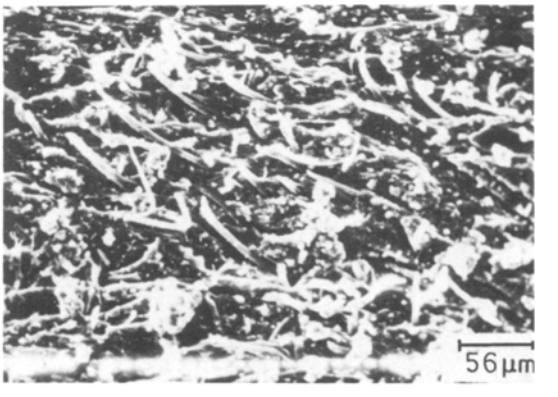

Figure 17 Scanning electron micrograph of the abraded surface of Mix D.

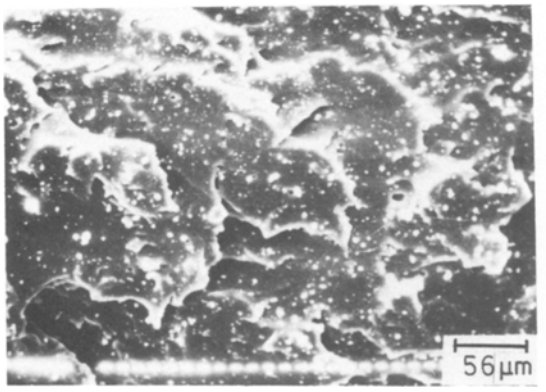

Figure 18 Scanning electron micrograph of the flex failed surface of Mix A.

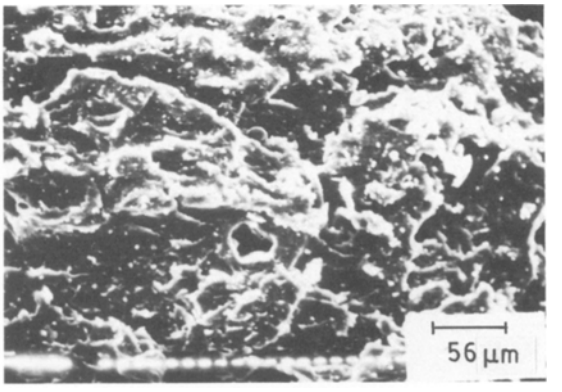

Figure 20 Scanning electron micrograph of the flex failed surface of Mix B.

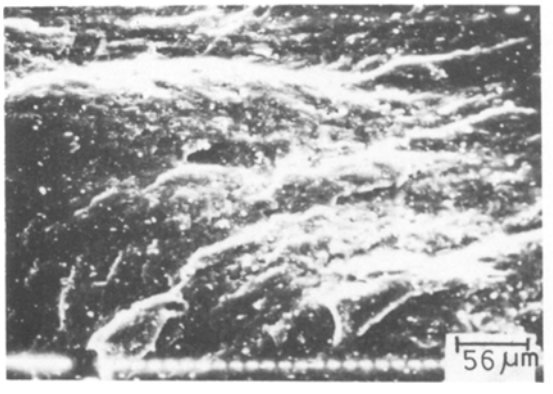

Figure 19 Scanning electron micrograph of the flex failed surface of Mix C.

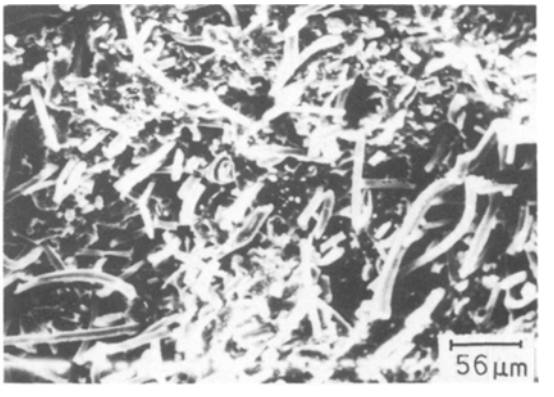

Figure 21 Scanning electron micrograph of the flex failed surface of Mix D.

shear failure with multidirectional cracks and grooves (Fig. 20).

Flex cracking resistance of short fibre-filled composite (Mix D) is very poor. Enhanced stiffness and hysteresis properties cause formation of deep cracks (Fig. 21). Repetitive cyclic deformations (from 0 to 180°) cause pulling out of the fibres from the rubber matrix. However, the extensive fibre breakage found on the fracture surface is due to breakage of the pulled out fibres during the course of flexing of the test specimens, and not due to breakage of the bonded fibres.

References

1. D. K. SETUA, S. K. CHAKRABORTY, S. K. DE and B. K. DHINDAW, *J. Scanning Electron Micros.* **3** (1982) 973.
2. N. M. MATHEW, A. K. BHOWMICK, B. K. DHINDAW and S. K. DE, *J. Mater. Sci.* **17** (1982) 2594.
3. N. M. MATHEW, A. K. BHOWMICK and S. K. DE, *Rubber Chem. Technol.* **55** (1982) 51.
4. D. K. SETUA and S. K. DE, *J. Mater. Sci.* **18** (1983) 847.
5. N. M. MATHEW and S. K. DE, *Int. J. Fatigue* January (1983) 23.
6. *Idem, J. Mater. Sci.* **18** (1983) 515.
7. D. K. SETUA and S. K. DE, *Rubber Chem. Technol.* **56** (1983) 808.
8. *Idem, J. Mater. Sci.* **19** (1984) 983.
9. S. K. CHAKRABORTY, D. K. SETUA and S. K. DE, *Rubber Chem. Technol.* **55** (1982) 286.
10. M. P. WAGNER, *ibid.* **49** (1976) 703.
11. *Idem, Rubber World* **164** (1971) 46.
12. M. Q. FETTERMAN, *Rubber Chem. Technol.* **46** (1973) 927.
13. P. K. PAL and S. K. DE, *ibid.* **55** (1983) 1370.
14. B. B. BOONSTRA, *Polymer* **20** (1979) 691.
15. G. KRAUS, "Reinforcement of Elastomers" (Interscience, Wiley, New York, 1965) p. 339.
16. A. I. MEDALIA, Proceedings of International Conference on "Structure property relations of rubber", Kharagpur, India, 20–31 December, 1980 (Indian Institute of Technology, Kharagpur, 1980).

17. E. M. DANNENBERG and J. J. BRENNAN, *Rubber Chem. Technol.* **39** (1966) 597.
18. A VOET, J. C. MORAWSKI and J. B. DONNET, *ibid.* **50** (1977) 342.
19. A. VOET, *J. Polym. Sci. Macromolecular Rev.* **15** (1980) 327.
20. P. R. JOHNSON, *Rubber Chem. Technol.* **49** (1976) 650.
21. V. M. MURTY and S. K. DE, *J. Appl. Polym. Sci.* **27** (1982) 4611.
22. A. Y. CORAN, P. HAMED and L. A. GOETTLER, *Rubber Chem. Technol.* **49** (1976) 1167.
23. A. Y. CORAN, K. BOUSTANY and P. HAMED, *J. Appl. Polym. Sci.* **15** (1975) 2471.
24. N. M. MATHEW and S. K. DE, *Polymer* **23** (1982) 632.
25. E. SOUTHERN and A. G. THOMAS, *Rubber Chem. Technol.* **52** (1979) 1008.

Received 16 July
and accepted 20 November 1984